DRAFT VERSION AUGUST 8, 2019
Typeset using LaTeX **twocolumn** style in AASTeX62

TYPE Ia SUPERNOVAE FROM NON-ACCRETING PROGENITORS

JOHN ANTONIADIS,[1,2] S. CHANLARIDIS,[2] GÖTZ GRÄFENER,[2] AND NORBERT LANGER[2,1]

[1]*Max-Planck Institut für Radioastronomie, Auf dem Hügel 69, 53121, Bonn DE*
[2]*Argelander Institut für Astronomie, Auf dem Hügel 71, 53121, Bonn DE*

Submitted to AAS Journals

ABSTRACT

We study the late evolution of two helium stars with masses of 1.8 and 2.5 $M_\odot$, considering the effects of electron captures, urca cooling. We demostrate that the mass of the core grows steadily and reaches the Chandrasekhar mass limit. Both models avoid electron capture reactions.

Keywords: supernovae: general – evolution stars: interiors

1. INTRODUCTION

Despite their central role in Astrophysics and Cosmology, the origin and physics of Type Ia supernova explosions (SNe Ia) remain uncertain (Maoz et al. 2014). The observed luminosities ($\geq 10^{43}\,\mathrm{erg\,s^{-1}}$) and ejecta velocities ($\sim 10^4\,\mathrm{km\,s^{-1}}$), imply ^{56}Ni masses and kinetic energies of order $\sim 0.6\,M_\odot$ and $\sim 10^{51}\,\mathrm{erg}$ respectively. These properties indicate that SNe Ia are most likely stars that disrupt in thermonuclear explosions, rather than core-collapse events. Carbon/oxygen white dwarfs (CO WDs) approaching the Chandrasekhar-mass limit ($M_{\rm Ch}$) are the most promising progenitor systems, as they can produce explosions broadly consistent with the inferred luminositites, energetics, compositions and delay times in respect to star formation (Arnett 1969; Nomoto 1982; Wang & Han 2012; Churazov et al. 2014).

Common stellar evolution channels produce stable CO WDs with masses below $\sim 1.0\,M_\odot$. Consequently, matter accretion onto the WD is required to trigger an explosion, either through stable mass transfer from a donor star (single-degenerate channels; SD), or in a merger event (double-degenerate channels; DD). Thus far, all of the proposed SD or DD variants encounter substantial difficulties in providing a self-consistent model for SNe Ia (Livio & Mazzali 2018). For instance SD channels require considerable fine-tuning of the mass accretion rate for the WD to grow in mass. In addition, the interaction of the SN blast with the donor star and the circumbinary material is expected to produce observable signatures which are rarely or never seen, e.g. some contribution to the SN bolometric luminosity at early times (Kasen 2010), long-lasting radio synchrotron emission (Harris et al. 2016), and possibly Hα emission due to unburned hydrogen. DD mergers on the other hand, may lead to a variety of outcomes, ranging from prompt explosions to long-lived remnants, or the delayed formation of a neutron star (Livio & Mazzali 2018). In addition, their overall contribution to the observed SN Ia rate may be too low (van Kerkwijk et al. 2010; Sato et al. 2015).

Over the past 50 years, systematic studies of SN Ia explosions have revealed a large diversity in their properties (Kirshner et al. 1973). Examples of outliers include luminous (e.g. SN 1991T; Filippenko et al. 1992) and ultra-luminous (e.g. SNLS-03D3bb; Howell et al. 2006) SNe, SN 1991bg-like transients which are faint and rapidly evolving (Ruiz-Lapuente et al. 1993), and SN 2012ca-like events, dubbed SNe Ia-CSM, in which there is evidence for interaction with a dense circum-stellar medium (Bochenek et al. 2018). Even among more "canonical" SNe Ia there is appreciable variance in rise times, maximum luminosities, ejecta velocities and spectral evolution (Mazzali et al. 2007; Livio & Mazzali 2018). Finally, there seems to be a correlation with environment, with active star-forming galaxies generally hosting more, and brighter SNe Ia (Pritchet et al. 2008).

While part of this diversity can be understood within the framework of SD and DD variants, it is likely that there exist additional evolutionary pathways leading to SNe Ia. In this work, we explore an alternative channel in which a thermonuclear runaway is initiated during the late evolution of stripped helium stars with neon-oxygen (NeO) or carbon-neon-oxygen (CNeO) cores and near-Chandrasekhar mass. These objects have been traditionally considered as potential progenitors of electron capture supernovae (ECSN) and accretion induced collapse (AIC) events (e.g., Nomoto & Kondo 1991; Gutierrez et al. 1996; Takahashi et al. 2013). However, recent hydrodynamical simulations indicate that if explosive oxygen burning is initiated at relatively low densities, the star may disrupt instead of imploding (Jones et al.

Corresponding author: John Antoniadis
janton@mpifr.de

2019). In addition, the presence of residual unburned carbon has been found to have an important influence on the energetics at late evolutionary stages (Willcox et al. 2016; Schwab & Rocha 2019). Here, we show that the evolution of intermediate-mass ($\sim 1.8 - 2.5\,M_\odot$) helium stars – a common product of binary interactions– naturally leads to the formation of near-Chandrasekhar (C)NeO cores that ingite carbon and oxygen explosively at low densities, before the onset of ^{20}Ne(e^-,ν_e)^{20}Fe electron capture reactions. In addition, the envelope is promptly lost via winds or in a common envelope episode, leaving behind a helium-free structure. We demonstrate that the combination of final composition and available energy, would yield explosions with luminosities and ejecta velocities consistent with classical SNe Ia. This mechanism does not require accretion from the binary companion and therefore may contribute significantly to the SN Ia rate at short delay times in respect to star formation.

The text is organized as follows. In Section 2 we briefly review the evolution of super-AGB stars and present our results for two representative helium-star progenitor models, evaluated using the *Modules for Experiments in Stellar Astrophysics* (MESA; Paxton et al. 2011, 2013, 2015, 2018). In Sectiosn 3 and 4, we provide estimates zeroth-order estimates for the energetics and SN Ia rates respectively. Finally, in Section **??** we conclude with a broader discussion on some possible implications and directions for future research.

2. (C)NeO CORES: FORMATION AND EVOLUTION

Highy degenerate stellar cores with neon-oxygen composition form inside stars with ZAMS masses between 7 and $11\,M_\odot$ (Farmer et al. 2015; Woosley 2019). After core helium burning, such stars enter a super-asymptotic giant branch (super-AGB) phase, characterized by a dense carbon-oxygen core and an extended hydrogen envelope. As the core becomes increasingly more degenerate, it cools substantially due emission of thermal neutrinos. An important consequence is that the critical temperature for ^{12}C ignition is first attained off-center, creating a convectively bound flame that propagates inwards, converting the chemical composition to primarily neon, oxygen, sodium and magnesium.

Carbon burning in super-AGB stars is affected by complex mixing processes due to a combination of inverse composition gradients, overshooting, semi-convection and rotation. The penetration of NeONaMg ashes into unburned regions, may have a significant impact on the propagation of the burning front. Mixing generally reduces the thermonuclear reaction rate, leaving behind substantial amounts of unburned carbon. In extreme cases, the flame can be quenched completely, resulting in a hybrid structure, with a carbon-oxygen core, surrounded by a neon-oxygen mantle (Denissenkov et al. 2013).

The subsequent evolution and final fate of the star depend critical on the competition between neutrino cooling due to the presence of ^{23}Na^{23}Ne and ^{24}Mg^{24}Na Urca pairs, and compressional heating due to accretion from the helium burning shell (Schwab et al. 2017). Super-AGB stars are subject to significant dredge-up and thermally unstable shell burning. These effects may impact substantially the ability of the core to grown in mass.

However, thermal pulses and dredge-up episodes do not occur when the hydrogen envelope is lost, e.g. due to a common envelope (CE) event in a binary system. In such a case, helium shell burning is stable, allowing the core to approach the Chandrasekhar mass limit. In what follows, we build detailed numerical models to investigate the combined effects of residual unburned ^{12}C, Urca cooling and constant mass accretion from shell burning, in the late evolution of (C)NeO cores that originate from helium stars.

2.1. *Numerical Calculations: Input Physics*

We use MESA version 10386 to follow the evolution of two helium-star models, M1 and M2, with masses of 2.4 and $1.8\,M_\odot$ respectively. The initial models have uniform compositions with $Y = 0.98$ and $Z = 0.02$ (solar abundances are taken from Grevesse & Sauval 1998). We employ a nuclear network that considers 43 isotopes, from ^{1}H to ^{58}Ni. Reaction rates are based on the `JINA reaclib v2.0` compilation (Cyburt et al. 2010). Electron screening factors and cooling rates from thermal neutrinos are evaluated as in Farmer et al. (2015), and references therein. Weak interaction rates are taken from Suzuki et al. (2016). Wind mass loss rates are calculated using the `Dutch` option in MESA (Paxton et al. 2013).

Our baseline convection model considers standard, thermohaline and semiconvectional mixing. Convective stability is evaluated using the Ledoux criterion. By default, MESA uses the standard MLT recipe by Cox & Giuli (1968) for standard convection. However, following carbon burning, both our models develop dynamically-unstable super-Eddington envelopes, causing numerical difficulties. For this reason, we decided to employ the "enhanced" MLT option available in MESA (Paxton et al. 2013), which artificially reduces the super-adiabatic gradient leading to enhanced convective energy transport efficiency. This allows us to follow the evolution of the core after carbon burning without interruptions. Upon experimentation, we found that this choice may impact slightly the size of the helium burning shell, and consequently the final masses. Nevertheless, we are confident that the main result is not affected. We further discuss the evolution of the envelope in Section **??**. The MLT mixing length parameter is set to $a_{\rm MLT} = 2.0$ for both models. For thermohaline and semiconvection we employ the Kippenhahn et al. (1980) and Langer et al. (1983) treatments respectively. In addition to the baseline mixing parameters, in M2, we also consider the effects of overshooting, adopting an efficiency of $f_{\rm ov} = 0.014$ across all convective boundaries, including the base of the carbon burning flame. While mixing at this interface may not occur in reality, we use this as a means to quench the flame before reaching the center. Other mixing processes such as rotation and thermohaline can lead to the same outcome for similar initial helium core masses (Farmer et al. 2015). The MESA inlists are publicly available. A more extended grid which explores a broad range of initial masses,

metallicities and overshooting parameters will be presented in an accompanying paper (Chanlaridis et al. 2019).

2.2. *Simulation results*

Figure 1 shows Kippenhahn diagrams for models M1 and M2, focusing on the evolution after core helium burning.

M1 first ignites carbon at mass coordinate $\sim 0.3\,\mathrm{M}_\odot$. The initial flame is followed by secondary flashes which propagate in both directions. The entire carbon burning phase lasts for about 40,000 yr. During most of this time, the star has $R \simeq 125\,\mathrm{R}_\odot$ and $\log_{10} T_{\rm eff} \simeq 3.75$.

2.3. *Late evolution and thermonuclear runaway*

3. ENERGETICS AND NUCLEOSYNTHESIS

some text

4. RATES AND DELAY TIMES

A useful proxy for the potential (C)NeO/SN Ia connection would be a comparison between the SN Ia occurrence rate, $\mathrm{n}_{\rm SN\,Ia}$, and the number of stripped near-Chandrasekhar mass (C)NeO cores, $n_\star$. Here, we provide a simple estimate based on first principles to demonstrate that the two may indeed be similar.

Starting with a stellar population of a given mass, to first order, $n_\star$ would be some fraction of the stars that will end up forming (C)NeO cores. Since the hydrogen envelope needs to be removed before the onset of core helium burning, these stars would also need to be members of close binary systems, thus:

$$n_\star \simeq f_{\rm bin} \times f_{\rm int} \times n_{\rm (C)NeO}. \quad (1)$$

Here, $f_{\rm bin} \simeq 0.7$ (Sana et al. 2012) is the stellar binary fraction, $n_{\rm (C)NeO}$ is the total number of stars with (C)NeO cores, and $f_{\rm int} \leq 1$ is an efficiency factor to account for the impact of binary interactions (see below). For binaries, the number of systems with ZAMS masses within a certain range (Figure 4) is:

$$n(m_1, m_2) dm_1 dm_2 = m_1^\alpha q^\kappa dm_1 dq, \quad (2)$$

where m_1 is the mass of the primary, here defined as the initially more massive star, $q \equiv m_2/m_1 \leq 1$ is the mass ratio, and a, κ depend on the initial mass function (IMF) and mass-ratio distribution respectively. Integrating, one finds:

$$N = \int_{m_{\rm min}}^{m_{\rm max}} \int_{q_1}^{q_2} m_1^\alpha q^\kappa dm_1 dq = f \frac{(m_{\rm min}^{\alpha+1} - m_{\rm max}^{\alpha+1})(q_1^{\kappa+1} - q_2^{\kappa+1})}{(\alpha+1)(\kappa+1)}, \quad (3)$$

where f is an appropriate normalization factor. Naively, one would expect the largest contribution from stars able to evolve to the SAGB in isolation, viz. stars with ZAMS masses between ~ 7 and $11\,\mathrm{M}_\odot$ (Farmer et al. 2015). Since accretion from a companion is not required to trigger an explosion, both primaries and secondaries (namely *all* 7–$11\,\mathrm{M}_\odot$ stars formed in binaries) can contribute to $n_\star$. Hence, one finds $(m_{\rm min}, m_{\rm max}) = (7, 11)\,\mathrm{M}_\odot; (q_1, q_2) = (0, 1)$ for the primaries (blue region in Figure 4), and $(m_{\rm min}, m_{\rm max}) = (11, 125)\,\mathrm{M}_\odot; (q_1, q_2) = (7/11, 1)$ for the secondaries (red region). For normalization, we consider all systems within $(m_{\rm min}, m_{\rm max}) = (0.1, 125)\,\mathrm{M}_\odot$. Adopting a Chabrier (2005) IMF with $a = -2.35$ for $m_1 \geq 1$ and a $q-$distribution with $k = -0.1$, as inferred for massive stars (Sana et al. 2012), Eq. 3 yields $n_{\rm (C)NeO} \times f_{\rm bin} \simeq 5.42 \times 0.7 = 0.0039$ stars per solar mass formed, with the largest contribution, $\sim 80\%$ coming from primaries. For $f_{\rm int} \simeq 1$, $n_\star$ would therefore exceed the number of SN Ia integrated over a Hubble time, $n_{\rm SN\,Ia} \simeq 0.0027\,\mathrm{M}_\odot{}^{-1}$.

However, $f_{\rm int}$ is most likely smaller than unity. Firstly, only a fraction of initial binary population will create naked helium stars. Most systems within the hatched regions of Figure 4 will transfer mass to their less massive companions after leaving the main sequence. For most cases, this process will be dynamically unstable, leading to the removal of the envelope, so naively, one would expect $f_{\rm int} \gtrsim 0.6$.

Following the stripping of the envelope, any subsequent interaction should be sufficiently delayed, for the core to grow substantially in mass. The post-CE orbital period distribution should generally favor close binaries. Consequently, only a small fraction of the population will have separations $\gtrsim 100\,\mathrm{R}_\odot$ to experience a second CE episode. Nonetheless, a number of more compact binaries that will undergo stable case BB Roche-lobe overflow (RLO), could still leave behind stripped (C)NeO cores of sufficiently high mass. For instance, the binary simulations of Tauris et al. (2015) produce a considerable number of (C)NeO proto-WDs with $m \simeq M_{\rm Ch}$ and practically no helium in their envelopes.

Considering the domonant uncertainties, one finds $0.2 \lesssim f_{\rm int} \lesssim 0.5$. Taking into account further ambiguities in the IMF and initial configurations, we conclude that $0.08 \lesssim n_\star/n_{\rm SN\,Ia} \lesssim 2$. Unsurprisingly, this is also consistent with the findings of detailed population synthesis studies for the occurrence rate of ECSNe (e.g. Jones et al. 2019)

Obviously, the above estimate does not consider all possible ways in which systems could move in and out of the hatched regions in Figure 4. Of particular importance may be interactions occurring before the helium-burning phase. For instance, there are roughly three times as many systems with a total mass larger than $7\,\mathrm{M}_\odot$ than there are stars within the hatched regions of Figure 4. A fraction of this population can contribute to the observed rate via Case A/B RLO.

Similarly, additional contributions may come from higher-order multiple systems and dynamical interactions in dense environments (see next section).

4.1. *Delay Time Distribution*

Besides the integrated number of SNe Ia, a property that is more challenging to match is the evolution of the SN Ia rate with Cosmic time. The time-dependent SN Ia rate following a burst of star formation, a.k.a the delay time distribution function, $\mathrm{DTD}(t)$, is generally modeled as a power law with index

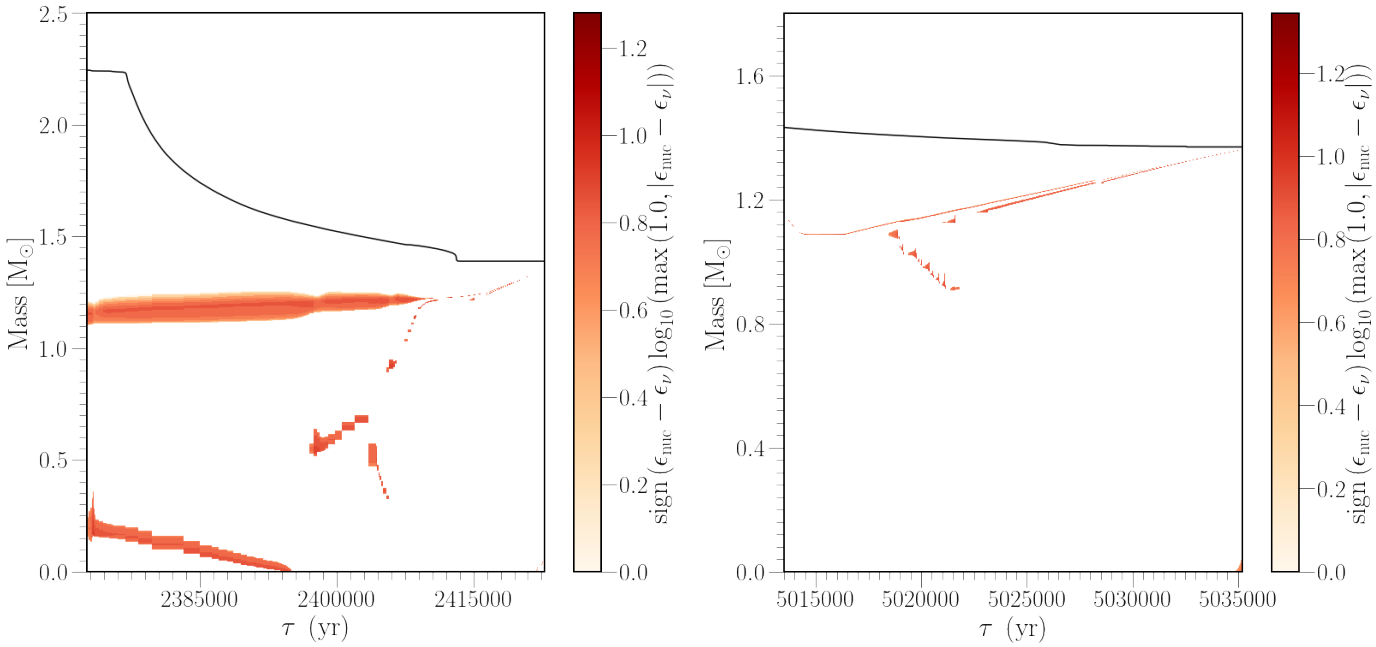

Figure 1.

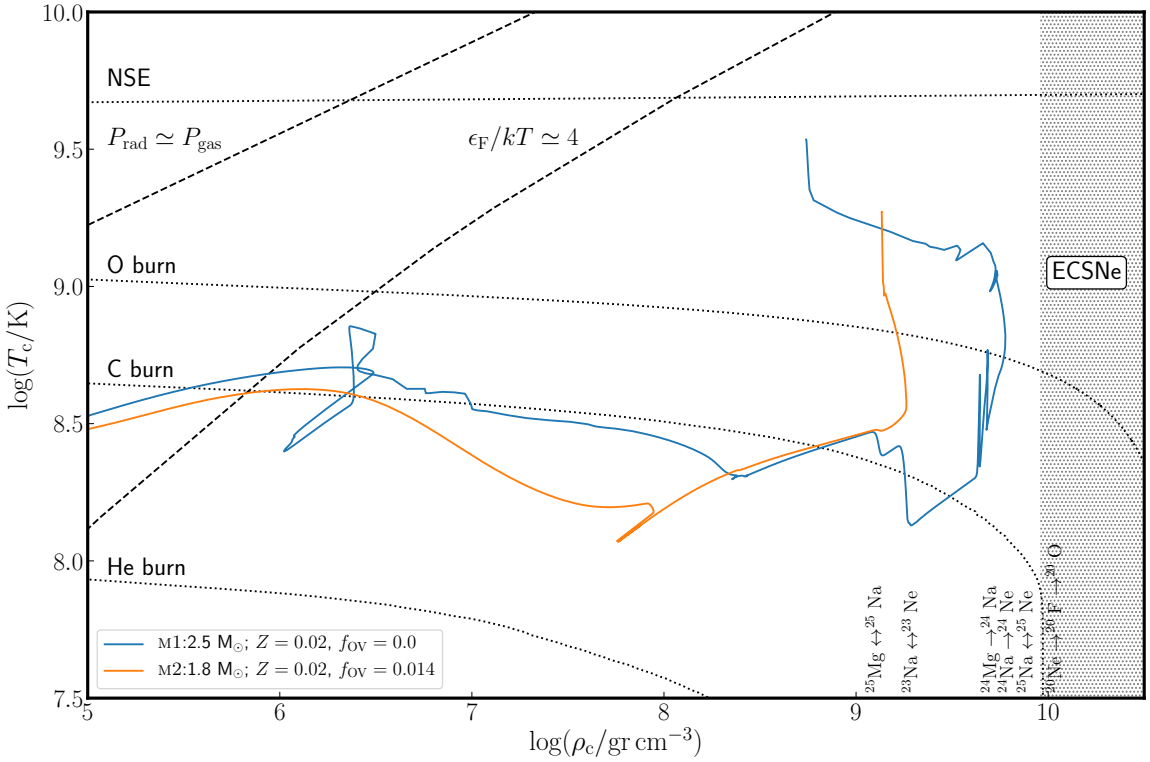

Figure 2. Evolution of the core density and temperature

5. DISCUSSION

We have shown that stars able to form degenerate (C)NeO cores after losing their hydrogen rich envelopes to binary in-

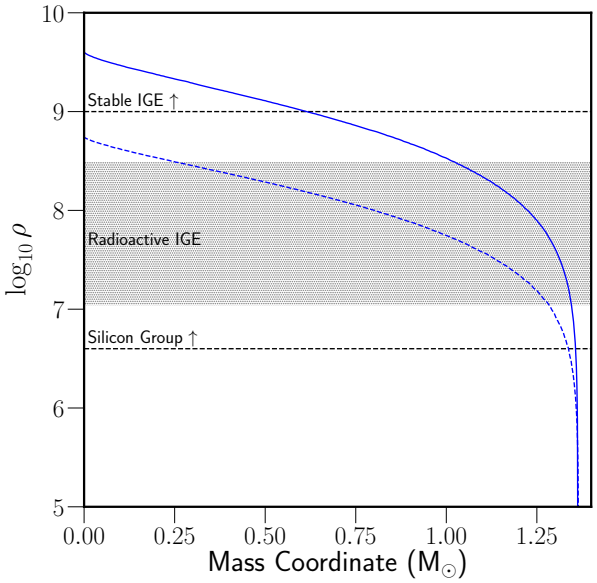

Figure 3. Density profiles

teractions, are likely to explode as SNe Ia instead of undergoing an ECSN and forming a neutron star (Sections 2 & 3). The frequency of these objects is sufficiently high to a count for a considerable fraction of the SN Ia occurrence rate (Section 4). **Götz & Norbert, would you be able to provide some input about MLT+, winds/velocities and possible WR-like properties of the progenitors?**

We thank Philipp Podsiadlowski, Friedrich Röpke, Samuel Jones and Josiah Schwab for useful discussions. This research made extensive use of NASA's ADS.

Software: MESA[1] (Paxton et al. 2011, 2013, 2015, 2018), Astropy[2] (Astropy Collaboration 2013; Astropy Collaboration & Astropy Contributors 2018) , mesaplot (Farmer 2018)

REFERENCES

Arnett, W. D. 1969, The Astrophysical Journal Supplement Series, 5, 180

Astropy Collaboration. 2013, Astronomy and Astrophysics, 558, A33

Astropy Collaboration, & Astropy Contributors. 2018, The Astronomical Journal, 156, 123

Bochenek, C. D., Dwarkadas, V. V., Silverman, J. M., et al. 2018, Monthly Notices of the Royal Astronomical Society, 473, 336

Chabrier, G. 2005, The Initial Mass Function 50 Years Later, 327, 41

Chanlaridis, S., Antoniadis, J., Gräfener, G., & Langer, N. 2019, in prep.

Churazov, E., Sunyaev, R., Isern, J., et al. 2014, Nature, 512, 406

Cox, J. P., & Giuli, R. T. 1968, Principles of stellar structure

Cyburt, R. H., Amthor, A. M., Ferguson, R., et al. 2010, The Astrophysical Journal Supplement Series, 189, 240

Denissenkov, P. A., Herwig, F., Truran, J. W., & Paxton, B. 2013, The Astrophysical Journal, 772, 37

Farmer, R. 2018, rjfarmer/mesaplot

Farmer, R., Fields, C. E., & Timmes, F. X. 2015, The Astrophysical Journal, 807, 184

Filippenko, A. V., Richmond, M. W., Matheson, T., et al. 1992, The Astrophysical Journal, L5

Grevesse, N., & Sauval, A. J. 1998, Space Science Reviews, 85, 161

Gutierrez, J., Garcia-Berro, E., Iben, I., et al. 1996, The Astrophysical Journal, 459, 701

Harris, C. E., Nugent, P. E., & Kasen, D. N. 2016, The Astrophysical Journal, 823, 100

Howell, D. A., Sullivan, M., Nugent, P. E., et al. 2006, Nature, 443, 308

Jones, S., Röpke, F. K., Fryer, C., et al. 2019, Astronomy and Astrophysics, 622, A74

Kasen, D. 2010, The Astrophysical Journal, 708, 1025

Kippenhahn, R., Ruschenplatt, G., & Thomas, H.-C. 1980, Astronomy and Astrophysics, 91, 175

Kirshner, R. P., Oke, J. B., Penston, M. V., & Searle, L. 1973, The Astrophysical Journal, 185, 303

Langer, N., Fricke, K. J., & Sugimoto, D. 1983, Astronomy and Astrophysics, 126, 207

Livio, M., & Mazzali, P. 2018, Physics Reports, 736, 1

Maoz, D., Mannucci, F., & Nelemans, G. 2014, Annual Review of Astronomy and Astrophysics, 52, 107

Mazzali, P. A., Röpke, F. K., Benetti, S., & Hillebrandt, W. 2007, Science, 315, 825

Nomoto, K. 1982, The Astrophysical Journal, 253, 798

[1] http://mesastar.org

[2] http://www.astropy.org

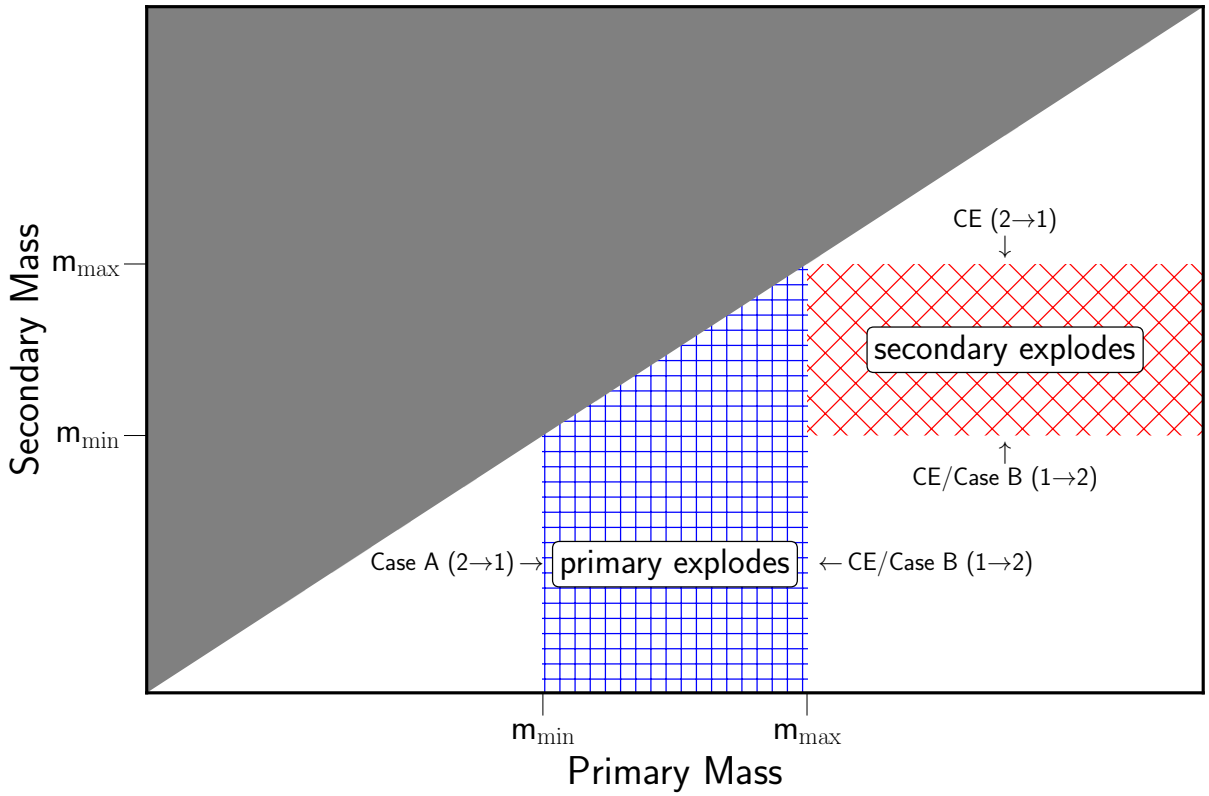

Figure 4. Evolution of core density and temperature

Nomoto, K., & Kondo, Y. 1991, The Astrophysical Journal, 367, L19

Paxton, B., Bildsten, L., Dotter, A., et al. 2011, The Astrophysical Journal Supplement Series, 192, 3

Paxton, B., Cantiello, M., Arras, P., et al. 2013, The Astrophysical Journal Supplement Series, 208, 4

Paxton, B., Marchant, P., Schwab, J., et al. 2015, The Astrophysical Journal Supplement Series, 220, 15

Paxton, B., Schwab, J., Bauer, E. B., et al. 2018, The Astrophysical Journal Supplement Series, 234, 34

Pritchet, C. J., Howell, D. A., & Sullivan, M. 2008, The Astrophysical Journal, 683, L25

Ruiz-Lapuente, P., Jeffery, D. J., Challis, P. M., et al. 1993, Nature, 365, 728

Sana, H., de Mink, S. E., de Koter, A., et al. 2012, Science, 337, 444

Sato, Y., Nakasato, N., Tanikawa, A., et al. 2015, The Astrophysical Journal, 807, 105

Schwab, J., Bildsten, L., & Quataert, E. 2017, Monthly Notices of the Royal Astronomical Society, 472, 3390

Schwab, J., & Rocha, K. A. 2019, The Astrophysical Journal, 872, 131

Suzuki, T., Toki, H., & Nomoto, K. 2016, \apj, 817, 163

Takahashi, K., Yoshida, T., & Umeda, H. 2013, The Astrophysical Journal, 771, 28

Tauris, T. M., Langer, N., & Podsiadlowski, P. 2015, Monthly Notices of the Royal Astronomical Society, 451, 2123

van Kerkwijk, M. H., Chang, P., & Justham, S. 2010, The Astrophysical Journal, 722, L157

Wang, B., & Han, Z. 2012, New Astronomy Reviews, 56, 122

Willcox, D. E., Townsley, D. M., Calder, A. C., Denissenkov, P. A., & Herwig, F. 2016, The Astrophysical Journal, 832, 13

Woosley, S. E. 2019, arXiv:1901.00215